

Boundary effects on modal shape in deep ocean via non-integer order parabolic cylinder functions

Jian-Kang Zhan(詹建康), Sheng-Chun Piao(朴胜春), and Li-Jia Gong(龚李佳)
Citation: Chin. Phys. B, 2026, 35 (**2**): 024303. DOI: 10.1088/1674-1056/ae1b7c
http://cpb.iphy.ac.cn; http://iopscience.iop.org/cpb

What follows is a list of articles you may be interested in

A WKB method based on parabolic cylinder function for very-low-frequency sound propagation in deep ocean

Jian-Kang Zhan(詹建康), Sheng-Chun Piao(朴胜春), Li-Jia Gong(龚李佳), Yang Dong(董阳), Yong-Chao Guo(郭永超), and Guang-Xue Zheng(郑广学)
Chin. Phys. B, 2025, 34 (**3**): 034301. DOI: 10.1088/1674-1056/ada886

Method for measuring the low-frequency sound power from a complex sound source based on sound-field correction in a non-anechoic tank

Hongzhe Xu(徐宏哲), Qi Li(李琪), Rui Tang(唐锐), and Dajing Shang(尚大晶)
Chin. Phys. B, 2023, 32 (**5**): 054303. DOI: 10.1088/1674-1056/acb75c

Three-dimensional acoustic propagation model for shallow waters based on an indirect boundary element method

Edmundo F. Lavia, Juan D. Gonzalez, and Silvia Blanc
Chin. Phys. B, 2023, 32 (**5**): 054301. DOI: 10.1088/1674-1056/ac90b1

A passive source ranging method based on the frequency warping transform of the vertical intensity flux in shallow water

Yu-Bo Qi(戚聿波), Shi-Hong Zhou(周士弘), Meng-Xiao Yu(于梦枭), Shu-Yuan Du(杜淑媛), Mei Sun(孙梅), Ren-He Zhang(张仁和)
Chin. Phys. B, 2019, 28 (**5**): 054302. DOI: 10.1088/1674-1056/28/5/054302

Influence of warm eddies on sound propagation in the Gulf of Mexico

Yao Xiao(肖瑶), Zhenglin Li(李整林), Jun Li(李鋆), Jiaqi Liu(刘佳琪), Karim G Sabra
Chin. Phys. B, 2019, 28 (**5**): 054301. DOI: 10.1088/1674-1056/28/5/054301

Boundary effects on modal shape in deep ocean via non-integer order parabolic cylinder functions

Jian-Kang Zhan(詹建康)[1,2,3], Sheng-Chun Piao(朴胜春)[1,2,3], and Li-Jia Gong(龚李佳)[1,2,3,†]

[1] *National Key Laboratory of Underwater Acoustic Technology, Harbin Engineering University, Harbin* 150001, *China*
[2] *Key Laboratory of Marine Information Acquisition and Security (Harbin Engineering University), Ministry of Industry and Information Technology, Harbin* 150001, *China*
[3] *College of Underwater Acoustic Engineering, Harbin Engineering University, Harbin* 150001, *China*

(Received 20 September 2025; revised manuscript received 1 November 2025; accepted manuscript online 5 November 2025)

This study investigates the effects of ocean boundaries on modal shapes in very-low-frequency (VLF, 1–10 Hz) sound propagation through the deep ocean. Utilizing a normal mode solution formulated in terms of parabolic cylinder functions (PCF), we demonstrate that boundary interactions induce a phase change reduction below $-\pi$ at frequencies of several hertz. This reduction, in turn, forces a key transition in the solution, shifting the order of the PCF from integer to non-integer values. Analysis of the characteristic shape of the PCF versus its order reveals that these boundary-influenced modes exhibit an energy shift toward deeper regions and a weakened axial convergence of the underwater sound field.

Keywords: very-low-frequency sound propagation, normal modes, parabolic cylinder function

PACS: 43.30.+m, 43.30.–k

DOI: 10.1088/1674-1056/ae1b7c **CSTR:** 32038.14.CPB.ae1b7c

1. Introduction

Very-low-frequency (VLF, 1–10 Hz) acoustic waves, characterized by wavelengths ranging from hundreds to thousands of meters, exhibit extraordinary propagation ranges of tens of thousands of kilometers in the deep ocean. This unique property holds significant application value in fields such as long-distance marine environmental monitoring,[1] underwater navigation, and geophysical research,[2] including the detection of seafloor earthquakes and tsunamis. The theoretical framework for modeling such wave propagation in horizontally stratified media often relies on the normal mode method, which decomposes the complex sound field into a sum of orthogonal eigenmodes, each with a distinct horizontal wavenumber and vertical modal shape.[3]

For sound propagation in the deep ocean, such as in the sound fixing and ranging (SOFAR) channel, traditional analysis frequently employs the Wentzel–Kramers–Brillouin (WKB) approximation to solve the modal equation. In this approach, the modal depth functions are typically constructed piecewise using trigonometric functions within the propagating region, with connection formulae handling the behavior near turning points.[4] This method has proven effective for higher frequencies. However, as the frequency drops into the VLF band (several hertz), the fundamental assumptions of the previous WKB approximation begin to break down. This requires the wavelength to be much smaller than the scale of the sound velocity variation, a condition that fails at VLF where wavelengths are comparable to the water depth. This failure limits the method's accuracy in characterizing the properties of VLF normal modes, necessitating more robust analytical solutions.

Furthermore, while ray-theoretic analyses have long indicated that ocean boundaries (surface and bottom) can influence the phase change experienced at a ray's turning point,[5] a clear and quantitative understanding of how these boundary conditions directly affect the shape of the normal modes themselves has remained elusive. Previous studies, such as those by Fitzgerald *et al.*,[6] have analyzed transmission loss and concluded that the most significant long-range paths are those avoiding bottom interaction (refracted-refracted paths). Nevertheless, the implicit boundary effects on these Rayleigh–Rayleigh (RR) modes, even without direct bottom interaction, and their consequent impact on the modal structure at VLF, have not been thoroughly investigated.

Addressing these gaps, this paper focuses on the critical role of ocean boundaries in shaping the VLF modal functions. We utilize a unified normal mode solution expressed in terms of parabolic cylinder functions (PCF),[7,8] which provides a continuous and accurate representation across the entire water column, including the turning points. This formulation allows us to move beyond the limitations of the piecewise WKB approach. The paper focuses on the critical role of non-integer-order PCF in VLF sound propagation, conveniently analyzing the influence of ocean boundaries on modal shapes under VLF conditions.

[†]Corresponding author. E-mail: lijia.gong@hrbeu.edu.cn

© 2026 Chinese Physical Society and IOP Publishing Ltd. All rights, including for text and data mining, AI training, and similar technologies, are reserved.

The paper is structured as follows. Section 2 presents the normal mode method based on PCF, clarifying the phase change-PCF order and modal shape relationship. Section 3 analyzes the impact of ocean boundaries on modal shape through simulations of a canonical deep-water sound velocity profile. Section 4 provides the conclusion.

2. Very-low-frequency normal modes express by parabolic cylinder functions in deep ocean

Building upon our previously established method for VLF sound propagation, which offers high accuracy and analytical advantages,[7,8] we derive the modal shapes using PCF. According to normal mode theory, the normalized normal modes in a waveguide can be obtained by

$$U_n(\xi_n,z) = \left.\frac{F_1(\xi,z)+\frac{1}{V_s(\xi)}\cdot\frac{F_1(\xi,0)}{F_2(\xi,0)}F_2(\xi,z)}{\sqrt{W(F_1,F_2)\frac{\partial}{\partial\xi}\left(\frac{1}{V_s(\xi)}\cdot\frac{F_1(\xi,0)}{F_2(\xi,0)}-V_b(\xi)\cdot\frac{F_1(\xi,H)}{F_2(\xi,H)}\right)}}\right|_{\xi_n}, \quad (1)$$

where $V_s(\xi)$ and $V_b(\xi)$ are the reflection coefficients from the surface boundary and bottom boundary, respectively.[9] The Wronskian W is given by

$$W(F_1,F_2) = F_1(\xi,z_s)F_2'(\xi,z_s) - F_1'(\xi,z_s)F_2(\xi,z_s). \quad (2)$$

The eigenvalue ξ_n is the n-th root of the dispersion equation

$$\frac{1}{V_s(\xi)}\cdot\frac{F_1(\xi,0)}{F_2(\xi,0)} - V_b(\xi)\cdot\frac{F_1(\xi,H)}{F_2(\xi,H)} = 0. \quad (3)$$

For a deep water waveguide with the Munk profile[10] as shown in Fig. 1, the linearly independent solutions $F_1(\xi,z)$ and $F_2(\xi,z)$ of the modal equation can be written using the uniform asymptotic approximation based on the PCF

$$F_1(\xi,z) = R(E)(S')^{-\frac{1}{2}}D_M(-y), \quad (4a)$$

$$F_2(\xi,z) = R(E)(S')^{-\frac{1}{2}}D_M(y). \quad (4b)$$

The function $D_M(y)$ is a parabolic cylinder function of order M, and

$$y = \sqrt{2}S(z), \quad (5a)$$

$$E(\xi_n) = \frac{2}{\pi}\int_{z_1(\xi_n)}^{z_2(\xi_n)}\sqrt{k^2(z)-\xi_n{}^2}\,\mathrm{d}z, \quad (5b)$$

$$M(\xi_n) = \frac{1}{\pi}\int_{z_1(\xi_n)}^{z_2(\xi_n)}\sqrt{k^2(z)-\xi_n{}^2}\,\mathrm{d}z - \frac{1}{2}, \quad (5c)$$

$$R(E) = 2^{\frac{1}{4}}\left(\frac{2e}{E}\right)^{\frac{E}{4}}. \quad (5d)$$

where $k(z)=\omega/c(z)$ is the wavenumber at depth z. $\omega = 2\pi f$ is the angular frequency, and f is the source frequency. z_1 and z_2 are the upper and lower turning points, and the function $S(z)$ is defined as

$$\begin{cases} \int_{s_1}^{S}\sqrt{\sigma^2-E}\,\mathrm{d}\sigma = \int_{z_1}^{z}\sqrt{\xi^2-k^2(z)}\,\mathrm{d}z, & 0\le z<z_1, \\ \int_{s_1}^{S}\sqrt{E-\sigma^2}\,\mathrm{d}\sigma = \int_{z_1}^{z}\sqrt{k^2(z)-\xi^2}\,\mathrm{d}z, & z_1\le z\le z_2, \\ \int_{s_1}^{s_2}\sqrt{E-\sigma^2}\,\mathrm{d}\sigma + \int_{s_2}^{S}\sqrt{\sigma^2-E}\,\mathrm{d}\sigma = \int_{z_1}^{z_2}\sqrt{k^2(z)-\xi^2}\,\mathrm{d}z + \int_{z_2}^{z}\sqrt{\xi^2-k^2(z)}\,\mathrm{d}z, & z_2<z\le H, \end{cases} \quad (6)$$

in which $s_1 = -\sqrt{E}$ and $s_2 = \sqrt{E}$.

Comparing Eq. (5c) with the WKB phase integral,[11] we can obtain the phase change δ_n of turning points for mode n as

$$\delta_n = 2\left(n - M_n - \frac{3}{2}\right)\pi, \quad n = 1,2,\ldots. \quad (7)$$

When analyzing the variation of the modal depth functions with depth z, according to Eq. (1), the denominator is independent of depth z and can therefore be treated as a constant. Each term in the numerator contains the factor $R(E)(S')^{-\frac{1}{2}}$, which can be regarded as an overall scaling factor for the modal shape. Thus, the modal depth functions can be simplified to

$$U_n(\xi_n,z) = A_n\left(D_{M_n}(-y) + \frac{1}{V_s(\xi_n)}\frac{D_{M_n}(-y)}{D_{M_n}(y)}\bigg|_{z=0}D_{M_n}(y)\right), \quad (8)$$

where A_n is depth independent. The above expression indicates that the modal shape depends solely on the shape of the PCF. Since the PCF shape is governed by its order M_n, the modal shape can therefore be expressed as a function of M_n. Consequently, the modal shapes under boundary effects can be investigated based on the order M_n of the PCF.

3. Results

This section compares the modal shapes under two cases to reveal the influence of ocean boundaries on VLF sound propagation: (i) the radiation condition commonly adopted in the SOFAR channel, where the turning points are well clear of the surface or bottom;[12] (ii) the waveguide with a pressure release surface and a penetrable fluid bottom, as detailed in Table 1.

Substituting the above boundary conditions into the dispersion Eq. (3) yields the eigenvalues ξ_n. However, the radiation condition involved in case 1 of this study actually corresponds to an unbounded environment. Therefore, we calcu-

lated the eigenvalues and eigenfunctions for this case according to Appendix B of Ref. [8]. Combining Eqs. (5c) and (7) gives the phase change δ_n and the order M_n of the PCF. We have computed the first and second modes based on these results, as shown in Fig. 2. From Figs. 2(a) and 2(b), we find that the phase velocity of mode 2 at 1 Hz exceeds the sound velocity, as shown in Fig. 1(b), leading to a bottom-interacting mode, which is beyond the scope of this study. The upper and lower turning point depths of the other modes lie between 0 and H, so they are all RR modes.

Table 1. Simulation conditions.

	Case 1	Case 2
Surface boundary	radiation condition, $U \to 0, z \to -\infty$	pressure release condition, $U = 0, z = 0$
Bottom boundary	radiation condition, $U \to 0, z \to +\infty$	fluid halfspace with $c_b = 1600$ m/s and $\rho_b = 1.6$ g/cm^3, $U + \rho_b / \sqrt{\xi^2 - \omega^2/c_b^2}\, U' = 0,\ z = H$

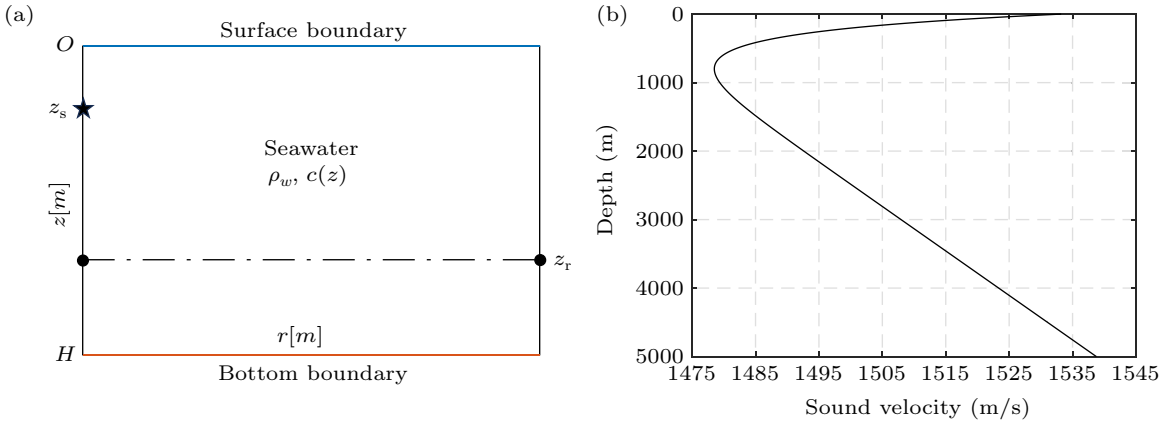


Fig. 1. (a) A deep water waveguide; (b) the Munk profile, which is expressed as $c(z) = c_a\{1 + \sigma[\exp(-\eta) + \eta - 1]\}$, where $\eta = 2(z - z_a)/b$. The specific parameters are $c_a = 1478.5$ m/s, $z_a = 800$ m, $b = 576$ and $\delta = 0.003$. This profile is used in the numerical simulations presented later.

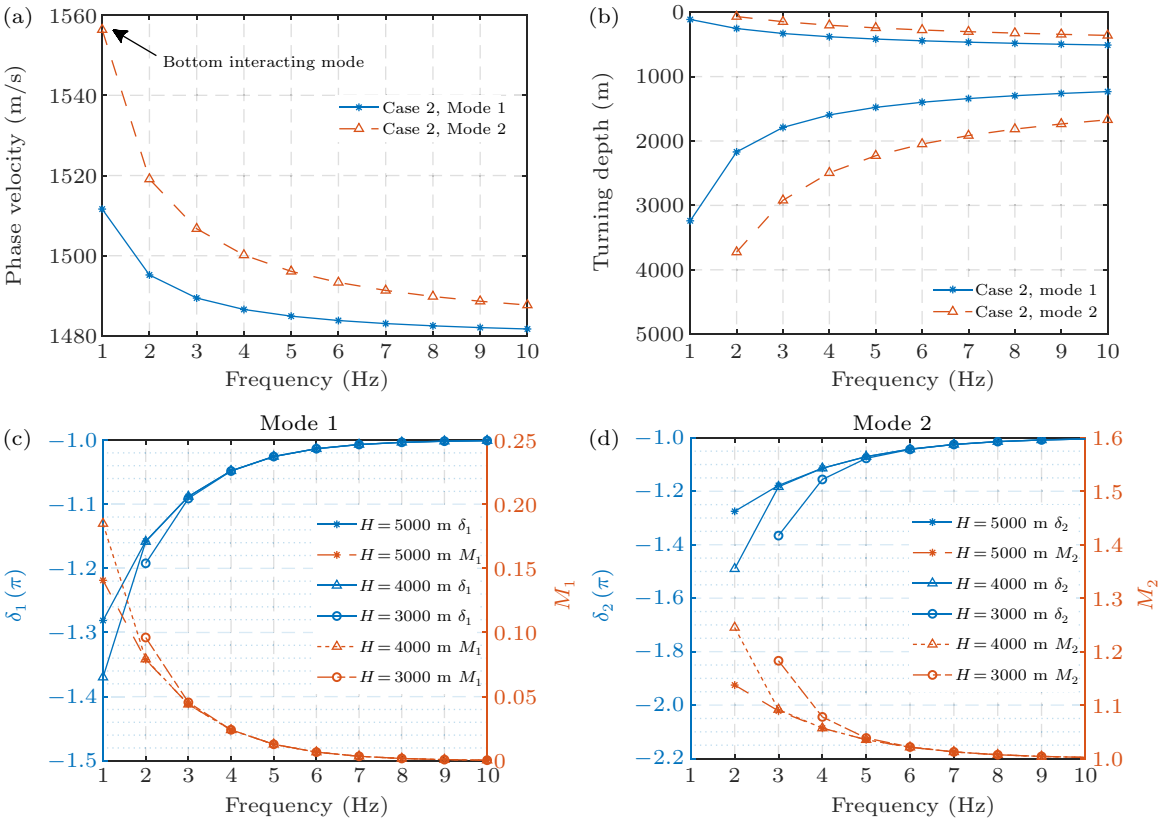


Fig. 2. Case 2: (a) phase velocities and (b) turning point depths for mode 1 and mode 2 when H is 5000 m; (c) phase change δ_1 and the PCF order M_1 for mode 1 under different water depths; (d) phase change δ_2 and the PCF order M_2 for mode 2 under different water depths.

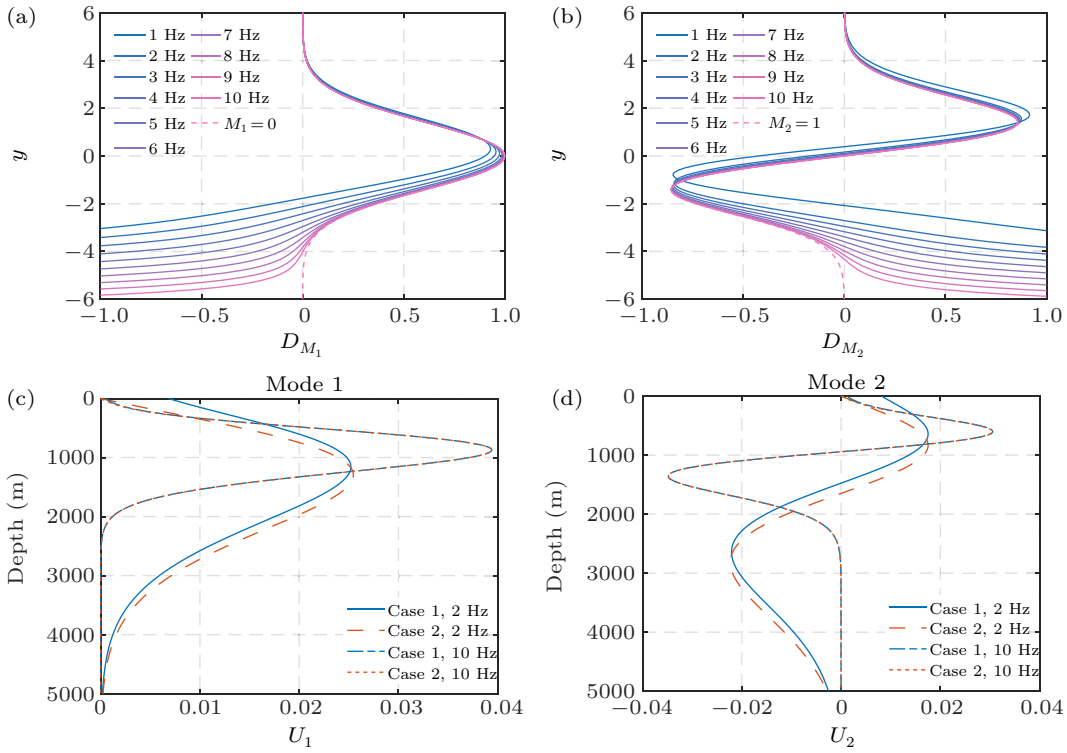


Fig. 3. (a) $D_{M_1}(y)$; (b) $D_{M_2}(y)$, the 1 Hz $D_{M_2}(y)$ corresponds to bottom interacting modes; (c) mode 1; (d) mode 2.

Under case 1, each turning point experiences a phase change of $-\pi/2$, resulting in a constant total phase change $\delta = -\pi$. This yields integer orders for the PCF. This corresponds to the classical ray theory, where rays undergo a $-\pi/2$ phase change at each turning point without boundary effects. However, as shown in Figs. 2(c) and 2(d), with decreasing frequency under case 2, the magnitude of the phase change δ_n for both mode 1 and mode 2 progressively decreases below $-\pi$. For example, at 1 Hz, $\delta_1 = -1.28\pi$ and $\delta_2 = -1.68\pi$. This indicates that the influence of ocean boundaries on the phase change intensifies as frequency decreases, consequently resulting in non-integer orders of the PCF (e.g., $M_1 = 0.14$ and $M_2 = 1.34$ at 1 Hz).

When the water depth changes, such as H being 3000 m and 4000 m, we analyze the impact of water depth on the phase change at the turning point and the order of the parabolic cylinder function under case 2. The results are shown in Figs. 2(c) and 2(d). The analysis indicates that the extent to which normal modes of different orders are affected by water depth differs significantly. For mode 1, when the water depth decreases from 5000 m to 3000 m, the phase change at the turning point and the corresponding order of the parabolic cylinder function begin to vary in the frequency band below 3 Hz. As the water depth decreases, both quantities exhibit an increasing trend. Above 3 Hz, however, the impact of water depth variation on these quantities is negligible. For mode 2, within the same range of water depth variation, the affected frequency band extends to below 5 Hz. Within this band, a similar increase in the phase shift at the turning point and the order of the parabolic cylinder function is observed as the water depth decreases. At frequencies above 5 Hz, both quantities remain largely unaffected by changes in water depth. Therefore, both ocean boundaries and water depth influence the phase change at the turning point and the order of the parabolic cylinder function, although this study focuses on the influence of ocean boundaries.

Next, when the water depth is 5000 m, since the shape of the PCF is governed by its order M, the transition from integer to non-integer values with decreasing frequency manifests directly in the evolving form of $D_{M_n}(y)$, as shown in Figs. 3(a) and 3(b). Under case 2, $D_{M_n}(y)$ progressively approaches the integer-order form $D_M(y)$ as the frequency increases from 1 Hz to 10 Hz. This demonstrates that the modal shape becomes increasingly influenced by ocean boundaries at lower frequencies, leading to alterations in the spatial energy distribution. For RR modes, Figs. 3(c) and 3(d) reveal that boundary effects significantly modify the 2 Hz modal energy distribution, and the case 2 peak position shifts toward the positive z-direction relative to its case 1 counterpart.

Furthermore, these alterations in modal shapes directly modify the spatial distribution of the sound field within 100 km. As shown in Fig. 4, the sound field distributions at 10 Hz are nearly identical for both cases, with the extreme point of transmission loss shifting by only about 10 m ($\approx 0.07\lambda$) in the positive z-direction. In contrast, a significant difference emerges at 2 Hz. Compared to case 1 (Fig. 4(c)),

case 2 exhibits not only a substantially deeper extreme point of transmission loss–located approximately 300 m (0.4λ) lower, but also a pronounced weakening of the axial acoustic energy convergence between 42–50 km (as indicated by the arrow). This weakening is attributed to a reduction in modal energy at the sound channel axis, as shown in Figs. 3(c) and 3(d).

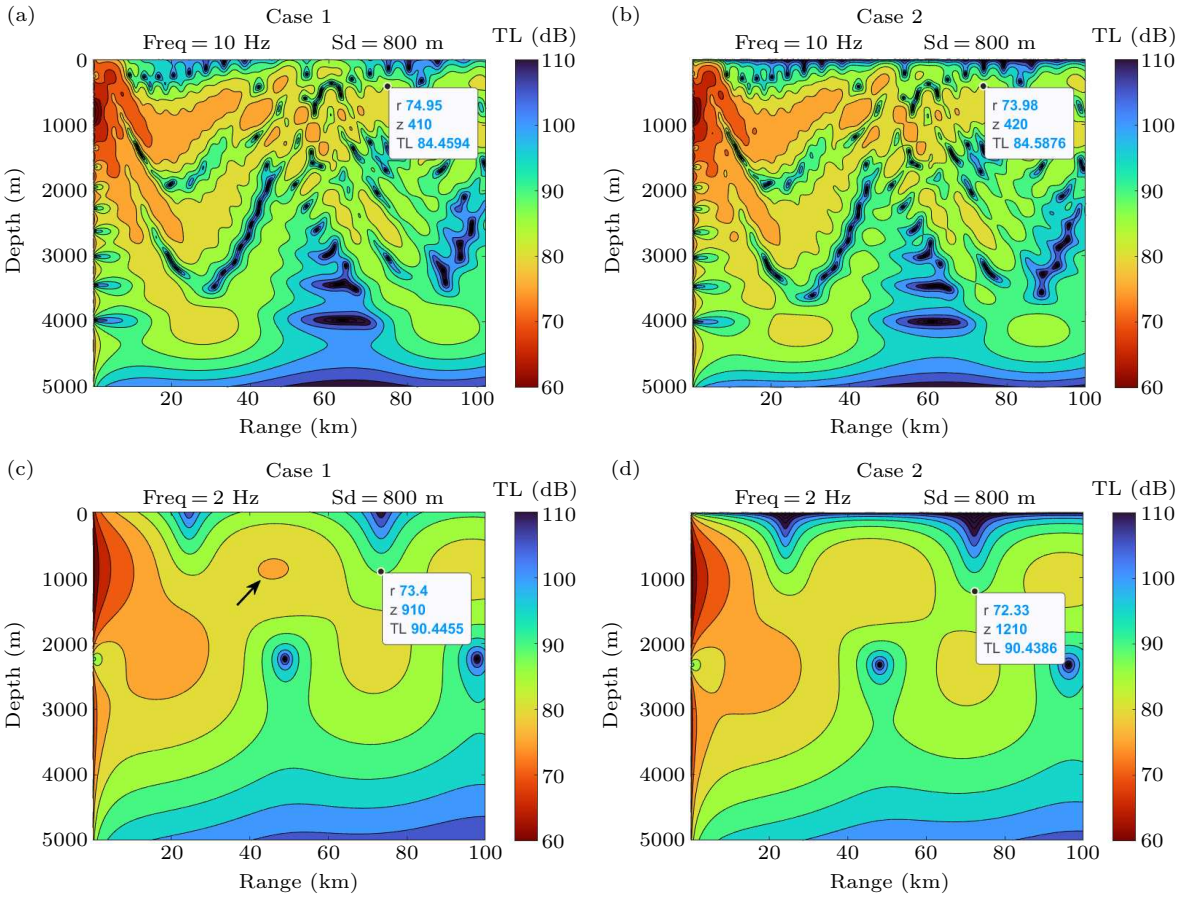


Fig. 4. Transmission loss of RR modes within 100 km: (a) case 1 at 10 Hz; (b) case 2 at 10 Hz; (c) case 1 at 2 Hz; (d) case 2 at 2 Hz.

4. Conclusion

This study systematically investigates the influence of boundary effects on modal shapes in VLF sound propagation based on the PCF solution to the normal modes. By establishing a PCF-based framework that links boundary conditions to continuous transitions in the PCF order, we elucidate the critical role of ocean boundaries in governing sound field mechanisms within the VLF band.

When frequencies decrease to several hertz, ocean boundaries significantly alter the phase change at the turning points for the modes, increasing its absolute value beyond π. This causes the PCF order to transition from integer to non-integer values, which directly modifies the spatial distribution of the modal depth functions. Consequently, modal energy shifts toward deeper water, and axial focusing of sound weakens. Therefore, the effects of surface and bottom boundaries must be taken into consideration in the SOFAR channel at several hertz.

However, the influence of elastic boundaries on the PCF order and the sound field affected by radiation into the bottom half-space has not yet been investigated.

Acknowledgment

Project supported by the National Natural Science Foundation of China (Grant No. 12204128).

References

[1] Eller A I, Heaney K D and Bradley D L 2023 *JASA Express Lett.* **3** 011001

[2] Oliveira T C A, Metz D, Lin Y T, Saragiotis C and Begnaud M L 2024 *J. Acoust. Soc. Am.* **155** 3371

[3] Jensen F B, Kuperman W A, Porter M B and Schmidt H 2011 *Computational Ocean Acoustics* (New York: Springer) pp. 143–147

[4] Zhang R H and Wang Q 1990 *J. Acoust. Soc. Am.* **87** 633

[5] Murphy E and Davis J 1974 *J. Acoust. Soc. Am.* **56** 1747

[6] Fitzgerald R, Shaffer J, Guthrie A, Nutile D and Hahn W 1979 *Long-Range, Deep-Ocean Propagation of 15-Hz CW Acoustic Signals* (Washington DC: Naval Research Lab)

[7] Piao S C and Zhan J K 2024 *Acta Acust.* **49** 784

[8] Zhan J K, Piao S C, Gong L J, Dong Y, Guo Y C and Zheng G X 2025 *Chin. Phys. B* **34** 034301

[9] Wang D Z and Shang E C 1981 *Underwater Acoustics*, 2nd edn. (Beijing: Science Press) pp. 63–66 (in Chinese)

[10] Munk W H 1974 *J. Acoust. Soc. Am.* **55** 220

[11] Harrison C H 2012 *J. Acoust. Soc. Am.* **132** 48

[12] Tindle C T 2002 *J. Acoust. Soc. Am.* **112** 464